

Observation of magnetization jump associated with a spin-state transition in oxygen-deficient $\text{Y}_{0.33}\text{Sr}_{0.67}\text{CoO}_{3-\delta}$

Yufeng Zhang, Sho Sasaki, Takano Odagiri, and Mitsuru Izumi

Laboratory of Applied Physics, Tokyo University of Marine Science and Technology, 2-1-6, Etchujima, Koto-ku, Tokyo 135-8533, Japan

(Received 5 September 2006; published 29 December 2006)

dc magnetization, electronic transport, and structural properties are studied on the mixed valence rare earth Sr-doped cobaltites $\text{Y}_{0.33}\text{Sr}_{0.67}\text{CoO}_{3-\delta}$. Oxygen deficiency and alternative layered structure with CoO_6 octahedron and CoO_4 tetrahedral polyhedron lead to the mixed valence states of Co ions. We found a Curie temperature at 304 K and a magnetization jump around 200 K under 0.01 T with a thermal hysteresis indicating a kind of magnetic memory effect. Temperature dependence of the electrical resistance exhibits nonmetallic with a thermal activation type. The observed magnetization jump is interpreted in term of a spin state transition of Co^{3+} ions in the octahedral site from the intermediate to low spin state. The intermediate spin configuration of Co^{3+} with $t_{2g}^5 e_g^1$ may develop an orbital ordering which accounts for the nonmetallic transport. With increasing magnetic field, the magnetization jump gradually disappears and its onset temperature shifts to lower temperature. The oxygen rich compound $\text{Y}_{0.33}\text{Sr}_{0.67}\text{CoO}_{2.704}$ with 6% rich Co^{3+} population compared to the less oxygen compound $\text{Y}_{0.33}\text{Sr}_{0.67}\text{CoO}_{2.614}$ shows a relatively large magnetization jump as well as the enhancement of the e_g electron localization leading to higher magnetic transition temperature from the intermediate to low spin state. Contrary, the less oxygen $\text{Y}_{0.33}\text{Sr}_{0.67}\text{CoO}_{2.614}$ shows the substantial low oxidation state as Co^{2+} which guides to a possible intermediate spin state stabilization.

DOI: 10.1103/PhysRevB.74.214429

PACS number(s): 75.60.Ej, 75.30.Sg, 75.25.+z, 71.70.Ej

INTRODUCTION

The transition-metal oxides with oxygen deficient superstructures of the basic perovskite ABO_3 have been extensively studied because of their rich physics and potential application in their behaviors of electrical transport and magnetic properties.^{1,2} The rare-earth strontium cobaltites $\text{RE}_{1-x}\text{Sr}_x\text{CoO}_3$ (RE is the rare-earth ion) have received lots of attention due to a couple of unique properties; namely, the existence of different Co spin states.³⁻⁵ i.e., high spin state, intermediate spin state, low spin state with different S in Co^{2+} , Co^{3+} , and Co^{4+} ions, as well as the unusual magnetic ground state of doped cobaltites.⁶⁻⁸ The physical properties of these materials are dependent upon the compositions as well as ionic and nonstoichiometric oxygen vacancy ordering. The cobaltites are composed of Co-O octahedral, tetrahedral, or both of them depending on the oxygen populations in the crystal structures.^{9,10} Comparatively, a series of cobaltates $\text{REBaCo}_2\text{O}_{5+\delta}$ exist with Co-O octahedral, pyramids or both structure under the different oxygen stoichiometry.^{7,11} It has been pointed out the oxides of high oxidation states lead to the change of the electronic structure, especially to a possible intermediate spin state stabilization.¹² The magnetization data of $\text{GdBaCo}_2\text{O}_{5+\delta}$ (Ref. 7) reveals a reentrant paramagnetic phase at 75 K, which was interpreted as a spin-state transition of the Co^{3+} ions in the octahedral site from the intermediate to low spin state. A part of the magnetization below 75 K comes from the contribution of Gd^{3+} ion which is magnetic. On the other hand, no paramagnetic behavior exists in YBaCo_2O_5 ¹³ down to low temperature because Y is nonmagnetic. The $\text{Y}_{1-x}\text{Sr}_x\text{CoO}_{3-\delta}$ family of compounds forms the single phase for compositions $x > 0.6$.^{14,15} Recently, Kobayashi *et al.*⁸ reported a room-temperature ferromagnetism with a Curie temperature of 335 K in $\text{Y}_{1-x}\text{Sr}_x\text{CoO}_{3-\delta}$ ($0.75 \leq x \leq 0.8$) due to the peculiar Sr/Y or

dering. The temperature dependence of the resistivity is nonmetallic which is ascribed as the antiferromagnetic state in the Co^{3+} orbital order. In cobaltites, the magnetic and electronic behaviors have been interpreted with the orbital ordering of Co^{3+} ions.^{7,8,11} Theoretical calculation by Korotin *et al.*¹⁶ on LaCoO_3 suggests that the intermediate spin configuration $t_{2g}^5 e_g^1$ is associated with a strong Jahn-Teller active state. Assuming the occupied e_g orbital order, the ordered intermediate spin state forms the ferromagnetic state in planes (001) under the antiferromagnetic coupling between planes. This accounts for the nonmetallic transport of LaCoO_3 at $90 \text{ K} < T < 500 \text{ K}$ well.

In this paper, we prepared $\text{Y}_{0.33}\text{Sr}_{0.67}\text{CoO}_{3-\delta}$ polycrystalline samples with different oxygen contents. The compounds induce a different population of spins with different mixed valence states of Co ions according to the existence of Co-O octahedral and tetrahedral coordinates. We found out a dc magnetization jump, the decrease in the magnitude around 200 K during the field cooling measurement under 0.01 T. Such discontinuous jump was observed with the only decreasing temperature and with increasing temperature the magnetization showed a relative small magnetization above the jump temperature followed from the lower temperature curve. The present magnetic phase transition indicating a kind of magnetic memory effect suggests a spin-state transition within a Co ionic site under the ferromagnetic ordering. The results are discussed with respect to the possible appearance of the spin states related to the oxygen deficiency.

EXPERIMENTS

Polycrystalline samples of $\text{Y}_{0.33}\text{Sr}_{0.67}\text{CoO}_{3-\delta}$ were prepared from stoichiometric mixtures of SrCO_3 (99.999%), Co_3O_4 (99.9%), and Y_2O_3 (99.99%) by the conventional solid state reaction. The mixtures were ground, pressed into a

pellet and calcined at 1100 °C for 48 h under the oxygen flow. The product was reground, pressed into a pellet and sintered at 1250 °C under flowing oxygen for two days until no further reaction was evident by the x-ray powder diffraction to obtain the oxygen-processed sample. The air-processed sample was prepared in air under the same temperature condition. As has been noted, the $Y_{1-x}Sr_xCoO_{3-\delta}$ family of compounds forms single phase for compositions $x > 0.6$.^{14,15} Room temperature x-ray diffraction measurements by the RIGAKU RADII-A diffractometer with Cu $K\alpha$ radiation verify the crystal structure and parameters around Co ions successfully. The refinement of the crystal structure for the obtained diffraction data was done by using a program RIETAN.¹⁷ dc magnetization was measured by quantum design SQUID magnetometer in the temperature range of 5 K–340 K under the magnetic field of 0–5 T. dc electrical resistance was measured by a four-probe method down to 10 K.

The oxygen content as well as chemical composition of doped Sr for Y is considered to have an important influence on the structural stability with electronic and magnetic states. The homogeneity and stoichiometry of the samples were analyzed by the electron-probe microanalysis (EPMA) and inductively coupled plasma (ICP) spectroscopy. The results confirmed that the molar ratio of Y:Sr:Co is 0.323:0.672:1 in the oxygen-processed sample and 0.337:0.707:1 in the air-processed sample, respectively. They are close to the nominal compositions. The oxygen content was determined through iodometric titration.¹⁸ Powdered sample 20 mg was dissolved in 6 M HCl solution (circa 5 ml) containing an excess KI (50%, circa 10 ml). The formed iodine of the stoichiometric amount was titrated with $Na_2S_2O_3$ solution using electrochemical reaction of AgCl and Pt electrode to detect the end point. The concentration of $Na_2S_2O_3$ solution was standardized against both KIO_3 and KI solution. To prevent oxidation by oxygen in air, the titration experiment was conducted under the Ar atmosphere flow. We repeated every experiment for three times and found the reproducibility. Eventually, the oxygen contents of both samples were obtained as $Y_{0.33}Sr_{0.67}CoO_{2.614}$ for the oxygen-processed sample and $Y_{0.33}Sr_{0.67}CoO_{2.704}$ for the air-processed sample, which suggested the existence of both Co^{2+} and Co^{3+} ions (see Table I).

RESULTS AND DISCUSSIONS

Powder x-ray diffraction profiles and Rietveld refinement procedure for the oxygen-processed $Y_{0.33}Sr_{0.67}CoO_{2.614}$ reveal the existence of the tetragonal structure with a space group of $I4/mmm$ (No. 139). The x-ray diffraction is coming from the elastic scattering process of charge density distribution with an x-ray electromagnetic wave and the number of electrons of Y ion is close to those of Sr ion. Therefore, we have taken a choice of the initial coordinations of both Y and Sr ions from the results of the neutron diffraction analysis in $Y_{0.33}Sr_{0.67}CoO_{3-\delta}$.¹⁰ The results of the refinement by using a program RIETAN are shown in Fig. 1 with the observed and calculated diffraction intensity profiles. The refined crystal structure and crystal parameters are given in Fig. 2 and Table

TABLE I. Crystal data for oxygen-processed $Y_{0.33}Sr_{0.67}CoO_{3-\delta}$ from the refinement with a program RIETAN in space group $I4/mmm$ using x-ray diffraction data at room temperature. The oxygen contents determined by an iodometric titration are shown together with averaged valence of Co.

$Y_{0.33}Sr_{0.67}CoO_{3-\delta}$	O ₂ -processed	Air-processed
a (Å)	7.616(0)	7.630(6)
c (Å)	15.274(1)	15.284(13)
V (Å ³)	885.93(5)	889.80(13)
$S/R_F/R_I$	2.8/4.70/5.54	3.2/4.74/4.86
Y:Sr:Co	0.323: 0.672:1	0.337: 0.707:1
$3-\delta$	2.614 (3)	2.704 (11)
Co valence	2.917	2.982

I, respectively. The lattice parameters are $a=7.616(2)$ Å and $c=15.275(5)$ Å. In the refined structure, there are two asymmetry occupations for the Co cations, Co1 and Co2 as summarized in Table II. Two kinds of Co-O coordination form the alternated layered structures of CoO_6 octahedron block and CoO_4 tetrahedral polyhedron block along the c axis. The present result is consistent with the previous results.^{9,10} There remains a small impurity phase of Y_2O_3 at about 29° in the x-ray diffraction. The magnetization of Y_2O_3 powder sample was measured separately and there was no specific contribution to the present study. The air-processed sample exhibits the similar structure to that of the oxygen-processed sample.

Table I shows that the lattice parameters of the air-processed $Y_{0.33}Sr_{0.67}CoO_{2.704}$ are longer than those of the oxygen-processed sample. This verifies that the oxygen content in the air-processed sample is larger than that in the oxygen-processed sample. This is confirmed with the oxygen contents determined by the chemical analysis as shown in Table I. The reason why the air-processed polycrystalline sample has a rich oxygen composition than that of the oxygen-processed sample is not clear in the present stage. It is worth to note that the present procedure is not an annealing but sintering process. Such peculiar oxidation is open for future study. In fact, other preparation studies in the different sintering temperatures for the same Y-Sr-Co-O compounds by using the identical technique exhibit that the oxygen process leads to the high oxygen content in comparison with the air-processed samples.¹⁹ We speculate that the Co^{2+} existence so as to more Co^{2+} and Co^{3+} double exchange in the oxygen prepared samples generally results in the lower oxygen content in the oxygen-processed sample than that in the air-processed sample.

As shown in Table II, the averaged Co2-O interatomic distance in the air-processed $Y_{0.33}Sr_{0.67}CoO_{2.704}$ is longer than that obtained in the oxygen-processed $Y_{0.33}Sr_{0.67}CoO_{2.614}$, while the averaged Co1-O bond distance is slightly smaller than that in $Y_{0.33}Sr_{0.67}CoO_{2.614}$. The air-processed $Y_{0.33}Sr_{0.67}CoO_{2.704}$ implies the relatively rich oxygen content which may result in the strong distortion leading to the different magnetic and electrical properties from the oxygen-processed sample. Following the bond valence sum

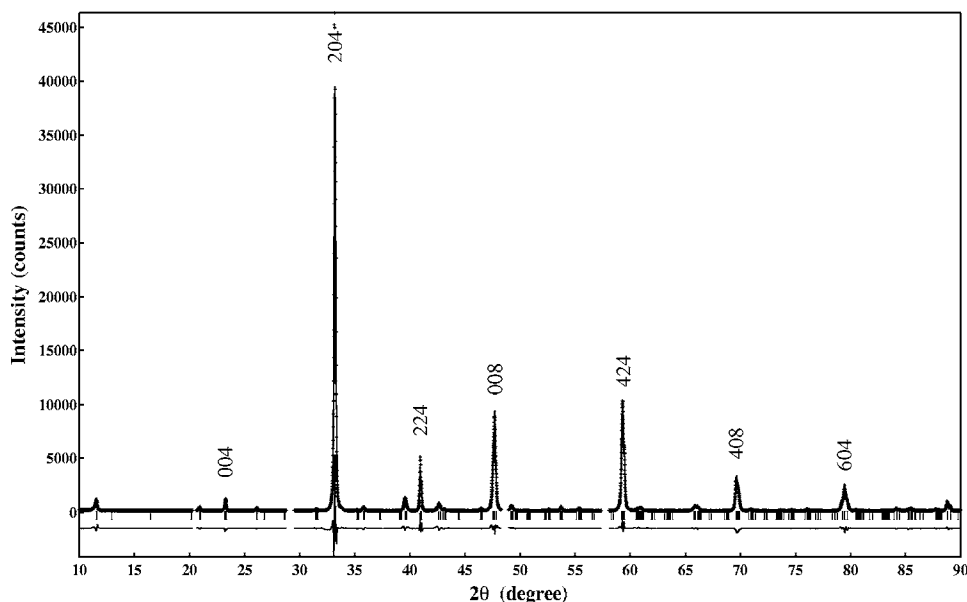


FIG. 1. X-ray diffraction intensity profiles of the oxygen-processed $Y_{0.33}Sr_{0.67}CoO_{2.614}$. The dotted curve indicates a collected intensity and the solid line is calculated with a least-square refinement by using a program RITAN. The lower trace shows the difference between calculated and experimental intensities.

calculations on $Y_{0.3}Sr_{0.7}CoO_{2.62}$,⁹ the samples showed that the tetrahedral site of Co1 was occupied by Co^{2+} and Co^{3+} ions and the octahedral site of Co2 was occupied with Co^{3+} ions only in the present polycrystalline samples. The calculation by using the chemical compositions, there are 4% Co^{2+} and 96% Co^{3+} on the tetrahedral site where 100% Co^{3+} on the octahedral site for the air-processed sample, and 16% Co^{2+} ion on the tetrahedral site and 100% Co^{3+} on the octahedral site in the oxygen-processed sample. The change in the number of Co ions with different oxidation number due to difference in the oxygen content induces the structural distortion so as to possibly relate to different magnetic and electronic transport properties.^{11,20,21} The air-processed $Y_{0.33}Sr_{0.67}CoO_{2.704}$ has 6% increased population of Co^{3+} compared to the population of Co^{3+} in the oxygen-processed $Y_{0.33}Sr_{0.67}CoO_{2.614}$.

Figure 3(a) shows the dc magnetization as a function of temperature for oxygen-processed sample (less Co^{3+}) under an applied static magnetic field of 0.01 T. There is a Curie temperature at 304 K below which the magnetization increases up to 280 K. This result shows a formation of ferromagnetic phase. There is an abrupt jump in the dc magnetization at 180 K, we define the temperature as T_J , upon decreasing temperature under the magnetic field in the oxygen-processed $Y_{0.33}Sr_{0.67}CoO_{2.614}$. Below 180 K, the magnetization shows the temperature independent magnetism associated with a possible small paramagnetic contribution down to 10 K. With increasing temperature, the dc magnetization monotonously increases and subsequently transit to the paramagnetic phase above 304 K. The result shows a thermal hysteresis, indicating a kind of magnetic memory effect as a function of temperature. To our knowledge, the present transition is reported in $Y_{0.33}Sr_{0.67}CoO_{3-\delta}$ for the first time. Magnetization jump was observed in the $GdVO_3$ single crystal along the a axis at about 8 K,²² which suggests the different domain arrangements in the homogenous antiferromagnetic phase. Cao *et al.*²³ also reported the magnetization step in $Pr_{5/8}Ca_{3/8}MnO_3$ manganites at low temperature which is possibly related to the spin quantum transition. Theoretical

calculation¹⁶ shows that the spin state transition from the intermediate to low spin state occurs at about 90 K in $LaCoO_3$. The magnetization increase at 75 K (Ref. 7) and 108 K (Ref. 11) in $GdBaCo_2O_{5+\delta}$ is explained to be accompanied with the spin-state transition of the Co^{3+} ions in the octahedral site from the intermediate to low spin state because the spin state of Co^{3+} ions in the square-pyramidal site may be high spin or intermediate spin state. The population of Co^{3+} ions is much larger than the Co^{2+} population in both samples, so we consider this phase transition at 180 K in $Y_{0.33}Sr_{0.67}CoO_{2.614}$ is most likely to be the spin state transition of Co^{3+} in the octahedral site from the intermediate to low spin state and magnetization drops instantly. With increasing temperature, another transition, the Curie temperature T_C , is observed at 304 K, which comes from the competition of the Co^{3+} orbital ordering state in the intermediate spin configuration between superexchange antiferromagnetic and ferromagnetic interactions. Similar phenomena appear in the air-processed $Y_{0.33}Sr_{0.67}CoO_{2.704}$ (rich Co^{3+}) as shown in Fig. 3(b). They show a Curie temperature at 304 K and the magnetization increases up to 280 K. The magnetization is larger than that in the oxygen-processed $Y_{0.33}Sr_{0.67}CoO_{2.614}$ with 6% less Co^{3+} population than the air-processed $Y_{0.33}Sr_{0.67}CoO_{2.704}$. Subsequently, below 280 K, we observe a substantial decrease to a magnetization jump at $T_J = 204$ K in the air-processed sample. The temperature of the magnetization jump is higher than that $T_J = 180$ K in the oxygen-processed sample, which deviates the conclusion¹² that a relative high oxygen state in the sample of $Y_{0.33}Sr_{0.67}CoO_{2.704}$ should stabilize the intermediate spin state. It is mainly due to the appearance of Co^{2+} ions in the samples and there is no Co^{4+} ion in the compounds which are different from the discussion of Ref. 12. It should be related that the oxides of the low oxidation states lead to the electronic structure modification, especially to a possible intermediate spin state stabilization. In $Y_{0.33}Sr_{0.67}CoO_{2.704}$, the increasing Co^{3+} ions due to oxygen deficiency induce larger magnetization and result in the strong Jahn-Teller distortion to localize the e_g electron²⁴ which increases the antiferro-

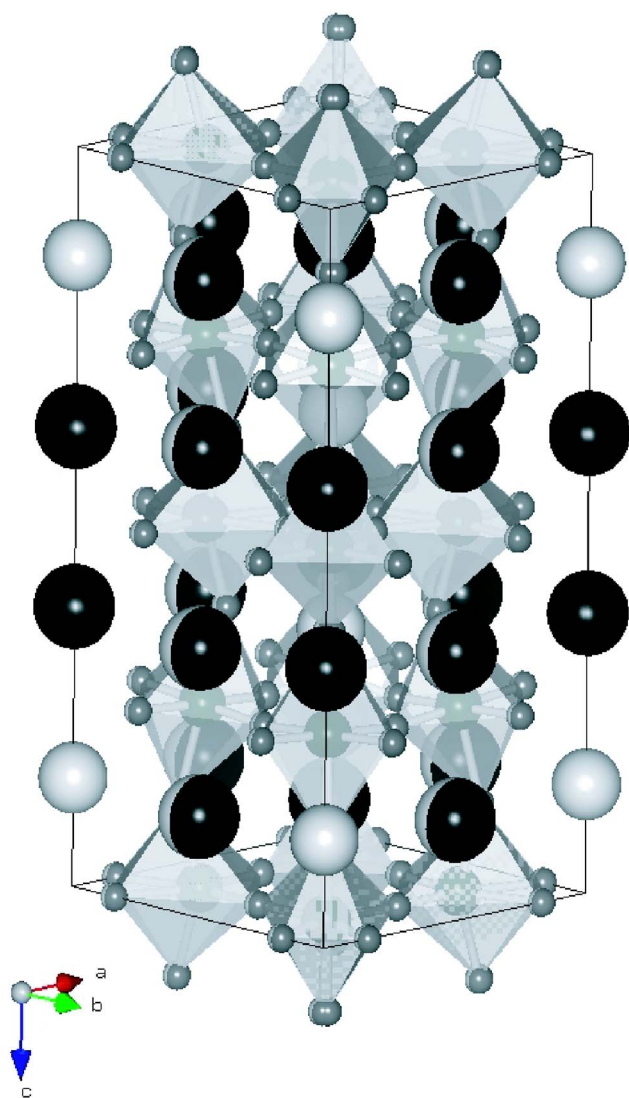


FIG. 2. (Color online) Crystal structure of the oxygen-processed $Y_{0.33}Sr_{0.67}CoO_{2.614}$ obtained from the Rietveld refinement of x-ray powder diffraction data by using a program RIETAN. The crystal symmetry is tetragonal with a space group $P4/mmm$; $a=7.616$ Å and $c=15.274$ Å.

magnetic interaction so as to the jump temperature and possibly weakens the intermediate spin state. The conjecture is also proved in the annealed samples of the oxygen-processed $Y_{0.33}Sr_{0.67}CoO_{2.614}$.

As shown in Fig. 4, the magnetization jump of the oxygen-processed $Y_{0.33}Sr_{0.67}CoO_{2.614}$ slowly vanishes and relative T_J shifts to the lower temperature from 180 K at 0.01 T to 164 K at 1 T. It indicates the “melting” of the orbital ordered antiferromagnetic state and the decrease of the ordering temperature which have been reported in manganites.²⁵ It is also shown in Fig. 4 that the magnetization increases around the low temperature with increasing the applied field, which may support the existence of the antiferromagnetic state at low temperature.

Figure 5 shows zero-field cooled magnetizations as a function of temperature for the oxygen-processed $Y_{0.33}Sr_{0.67}CoO_{2.614}$ under the applied magnetic field of

TABLE II. Interatomic distances between Co and oxygen ions in $Y_{0.33}Sr_{0.67}CoO_{3-\delta}$.

$Y_{0.33}Sr_{0.67}CoO_{3-\delta}$	O ₂ -processed	Air-processed
Tetrahedron		
Co1-O1(×2)	1.857(7)	1.814(11)
Co1-O2(×2)	1.961(12)	1.978(17)
Co1-O3(×2)	1.921(5)	1.911(8)
⟨Co1-O⟩	1.913	1.901
Octahedron		
Co2-O1(×1)	2.057(8)	2.144(15)
Co2-O4(×4)	1.909(0)	1.911(1)
⟨Co2-O⟩	1.983	2.028

0.01 T and 0.5 T, respectively. There is a cusp below 304 K at 0.01 T, which is related to glassiness²⁶ or spin glasslike.²⁷ With the magnetic field increasing to 0.5 T, the cusp temperature is still around 304 K, which suggests the cusp should be attributed to glassiness,²⁰ the system appears to contain the ferromagnetic clusters in an antiferromagnetic matrix. It is postulated that the competed phase separation of Co^{3+} ion ferromagnetic interaction and antiferromagnetic superexchange interaction induces the appearance of the cusp around T_C .

For studying the character of the difference magnetic transition temperature, we measured the dc magnetizations as a function of applied field for the oxygen-processed $Y_{0.33}Sr_{0.67}CoO_{2.614}$ at 285 K, 190 K, and 10 K, for the air-processed $Y_{0.33}Sr_{0.67}CoO_{2.704}$ at 295 K, 210 K, and 10 K, as

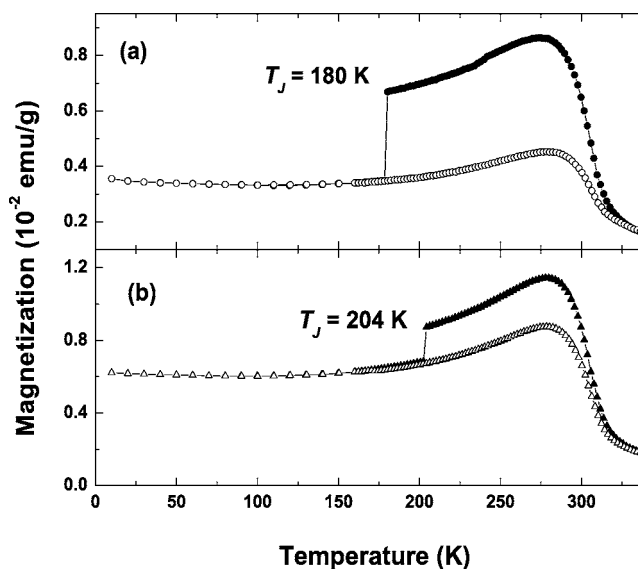


FIG. 3. (a) Magnetization as a function of temperature of the oxygen-processed $Y_{0.33}Sr_{0.67}CoO_{2.614}$ measured with decreasing temperature under magnetic field of 0.01 T (solid circles) and increasing temperature (open circles); (b) temperature dependence of magnetization of the air-processed $Y_{0.33}Sr_{0.67}CoO_{2.704}$ (triangles) under 0.01 T. The field cooling curve is shown as the solid symbols, whereas the field warming curve is shown as the open symbols.

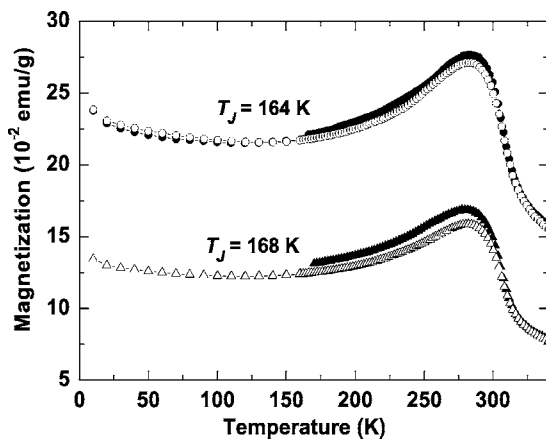


FIG. 4. Temperature dependence of magnetization of oxygen-processed $Y_{0.33}Sr_{0.67}CoO_{2.614}$ under 0.5 T (triangles) and 1 T (circles), respectively. The field cooling curves are shown as the solid symbols, whereas the field warming curves are shown as the open symbols.

shown in Figs. 6(a) and 6(b). The existence of the hysteresis loop for the air-processed sample at 295 K and 210 K implies a ferromagnetic component, suggesting a kind of ferromagnetic material; the lack of saturation will correlate with the antiferromagnetism.²⁰ The ferromagnetic clusters within an antiferromagnetic matrix are the most likely model here, which consists of the orbital ordering state mentioned. There are no hysteresis loop and saturation for $Y_{0.33}Sr_{0.67}CoO_{2.704}$ at 10 K, which indicates the antiferromagnetism of the low spin state at low temperature. For the oxygen-processed sample, there exists only a small hysteresis at 285 K and no hysteresis at other temperatures. The antiferromagnetic interaction is stronger than the ferromagnetic exchange in the Co^{3+} orbital ordering state so that the magnetic field dependence of the dc magnetization exhibits antiferromagnetic.

We measured the temperature dependence of the dc electrical resistance of the oxygen-processed $Y_{0.33}Sr_{0.67}CoO_{2.614}$

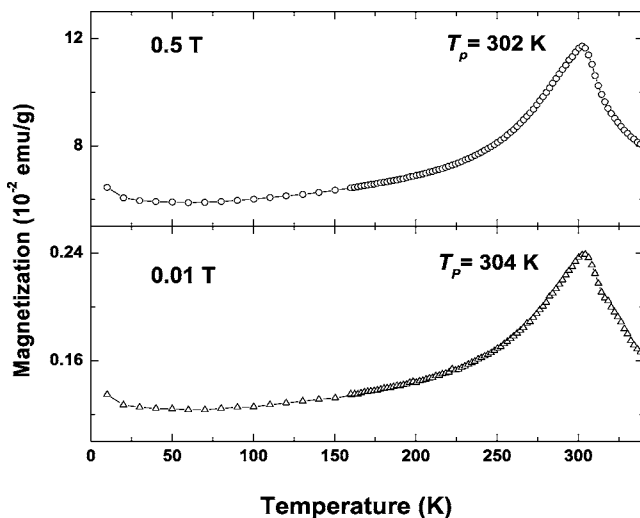


FIG. 5. Zero-field cooled magnetization as a function of temperature for the oxygen-processed $Y_{0.33}Sr_{0.67}CoO_{2.614}$ under fields of 0.01 T and 0.5 T.

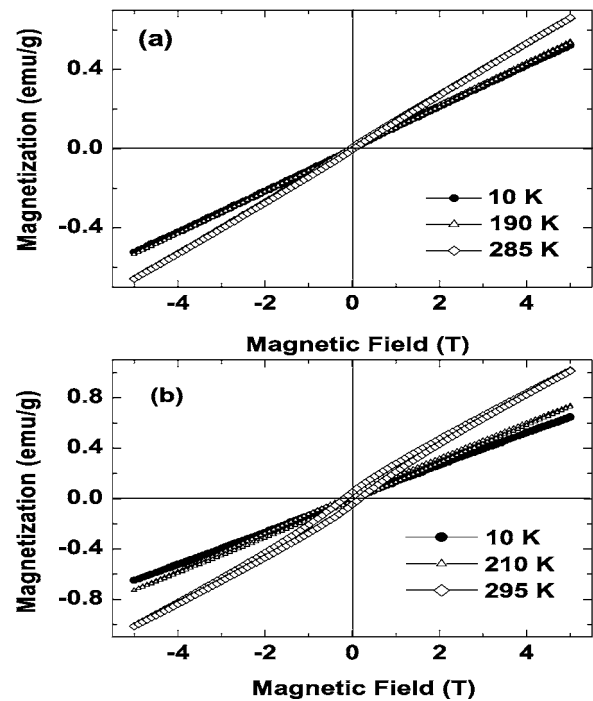


FIG. 6. (a) Magnetization curves as a function of magnetic field for oxygen-processed $Y_{0.33}Sr_{0.67}CoO_{2.614}$ at 285 K, 190 K, and 10 K. (b) Magnetization curves as a function of magnetic field for air-processed $Y_{0.33}Sr_{0.67}CoO_{2.704}$ at 295 K, 210 K, and 10 K.

(a) and the air-processed $Y_{0.33}Sr_{0.67}CoO_{2.704}$ (b) under zero magnetic field down to 115 K below room temperature. Figure 7 shows the electronic transport of both samples. The obtained results follow with the thermal activation-type $\rho = \rho_0 \exp(-\frac{\Delta}{k_B T})$ which suggests nonmetallic, where Δ is the activation energy. They are interpreted in the term of the appearance of the Co^{3+} ions with an orbital order in the intermediate spin state.¹⁶ The obtained activation energies are

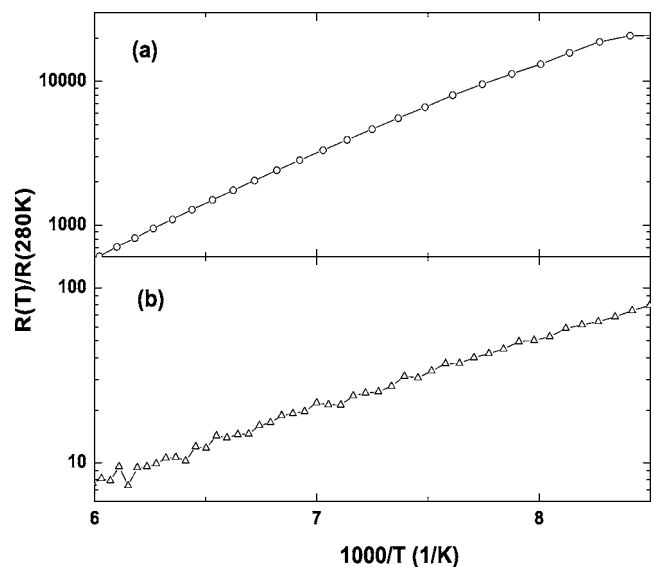


FIG. 7. Normalized dc electrical resistance as a function of temperature for both oxygen-processed $Y_{0.33}Sr_{0.67}CoO_{2.614}$ (a) and air-processed $Y_{0.33}Sr_{0.67}CoO_{2.704}$ (b).

approximately 0.33 eV for the air-processed $\text{Y}_{0.33}\text{Sr}_{0.67}\text{CoO}_{2.704}$ and 0.6 eV for the oxygen-processed $\text{Y}_{0.33}\text{Sr}_{0.67}\text{CoO}_{2.614}$ below room temperature. Obviously, it is rather incompatible with the double-exchange interaction because Co^{2+} ions in $\text{Y}_{0.33}\text{Sr}_{0.67}\text{CoO}_{2.614}$ are more than that in $\text{Y}_{0.33}\text{Sr}_{0.67}\text{CoO}_{2.704}$ with 6% increase of Co^{3+} population, which induces the stronger exchange interaction with Co^{3+} to reduce the thermal activation gap. From the magnetic measurement results, due to relatively rich Co^{3+} ions population the air-processed $\text{Y}_{0.33}\text{Sr}_{0.67}\text{CoO}_{2.704}$ exhibits the larger magnetization in the intermediate spin state which may decrease the activation energy. So the oxygen rich $\text{Y}_{0.33}\text{Sr}_{0.67}\text{CoO}_{2.704}$ possesses the lower activation energy than that of the oxygen less $\text{Y}_{0.33}\text{Sr}_{0.67}\text{CoO}_{2.614}$.

From the above the experimental results, it can be concluded that the magnetic memory effect of $\text{Y}_{0.33}\text{Sr}_{0.67}\text{CoO}_{3-\delta}$ compounds arises from the Co^{3+} spin state transition in the octahedral site from the intermediate to low spin state at a certain temperature. The formation of the orbital order interprets the nonmetallic property in the electronic transport.^{7,16} For $\text{Y}_{0.33}\text{Sr}_{0.67}\text{CoO}_{3-\delta}$ samples, the ferromagnetic properties above the T_J suggest that the electron ordering of Co^{3+} ions should be ascribed to the orbital ordering and not the charge ordering. There exists the alternative layered structure of the octahedral and tetrahedral with different Co-O bond length due to oxygen deficiency in the samples. This crystal structure is crucial to the ordering of the orbital of Co^{3+} . The intermediate spin state configuration is $t_{2g}^5 e_g^1$ with the strong Jahn-Teller active state. By the x-ray diffraction data in the powder form and the single-crystal of LaCoO_3 ,²⁸ the alternation of short and long bands in the a - b plane indicates the presence of e_g orbital ordering in the intermediate spin state induced by a cooperative Jahn-Teller distortion. The experimental results of Chernenkov *et al.* on $\text{GdBaCo}_2\text{O}_{5.5}$ (Ref. 29) indicate that the e_g electrons of Co^{3+} in the pyramidal site should have $d_{x^2-y^2}$ and $d_{3z^2-r^2}$ orbitals, which induce the high spin state; the e_g electron of Co^{3+} in the octahedral site should have $d_{x^2-z^2}$ and $d_{y^2-z^2}$ orbital, which are related to the intermediate spin state. The oxygen deficiency of $\text{REBaCo}_2\text{O}_{5.5}$ forms the rare earth RE^{3+} and Ba^{2+} order into alternative, thus the intermediate spin or high spin Co^{3+} state in the square-pyramidal site is stabilized with removing the oxygen of the RE^{3+} planes.³⁰ It supports our conclusions that the spin state transition from the intermediate to low spin state in the Co^{3+} among the octahedral coordinates results in the dc magnetization jump at a certain temperature and not in the tetrahedral positions. Based on the orbital order analysis by the x-ray diffraction on $\text{GdBaCo}_2\text{O}_{5.5}$ (Ref. 29) and the theoretical calculation on the Co^{3+} intermediate spin state of LaCoO_3 ,¹⁶ the spin mode of the e_g occupied orbital ordering of Co^{3+} ions in two dimensional sublattices can be crudely illustrated as shown in Fig. 8. As a starting point in octahedral site, we assign the e_g orbital $d_{y^2-z^2}^\uparrow$ of Co ions marked in the Oc11 and Oc12 (Oc: Octahedron). One e_g orbital is empty and t_{2g} orbitals are occupied with excluding d_{yz}^\downarrow based on the minimized Coulomb interaction energy concerning the e_g and t_{2g} electrons. For the neighboring Co ions, the $d_{x^2-z^2}^\uparrow$ orbital of the e_g electron is placed in the site Oc21 and Oc22 and the d_{xz}^\downarrow orbital is in the t_{2g} hole. Therefore, all the

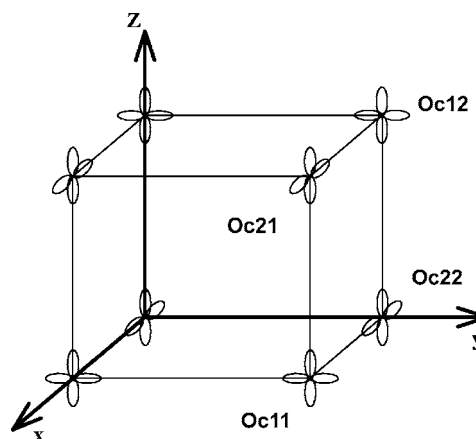


FIG. 8. A model of spin-state and orbital ordering in the intermediate spin state for the occupied e_g orbital of Co^{3+} ions in the octahedral site (Oc11–Oc22).

octahedral Co^{3+} ions are in the intermediate spin state and formed into the orbital ordering. It may be noted that such a spin structure supports the fact that there are in-plane ferromagnetic interaction and interplane antiferromagnetic coupling. Spin order arrangement of a similar kind have been also reported by Roy *et al.*¹¹ and Khomskii *et al.*³¹

There may exist a competition between the in-plane ferromagnetic interaction and interplane antiferromagnetic interaction with applied magnetic field and the ferromagnetic interaction overcomes antiferromagnetic superexchange interaction establishing a long range ferromagnetic state at $180 \text{ K} \leq T \leq 304 \text{ K}$ and a cusp with $T_C = 304 \text{ K}$ (see Fig. 5). The magnetization decrease below 280 K suggests the gradual antiferromagnetic appearance in the intermediate spin state. With decreasing temperature, there is a temperature tunable magnetization jump which accompanies with the spin state transition of the octahedral Co^{3+} ions from the intermediate to low spin state. In the low spin state, there should be no magnetization due to the $t_{2g}^6 e_g^0$ configuration and Y ion is nonmagnetic.¹³ However, a substantial magnetization in the low temperature accounts for that the Co^{3+} ion in the tetrahedral site may be in either the high spin or the intermediate spin states in whole temperature range.^{7,29} High magnetic field destroys the Co^{3+} antiferromagnetic state to favor ferromagnetism and both samples suggest the ferromagnetism. The orbital ordering corresponds to the antiferromagnetic ground state, so that the electrical resistance exhibits nonmetallic.^{8,16,32}

The 6% rich Co^{3+} ions in air-processed $\text{Y}_{0.33}\text{Sr}_{0.67}\text{CoO}_{2.704}$ than in $\text{Y}_{0.33}\text{Sr}_{0.67}\text{CoO}_{2.614}$ result in the higher magnetization and a relatively large Jahn-Teller distortion which localizes the e_g electron to increase the jump temperature.

CONCLUSIONS

In summary, the structural and magnetic properties of the air- and the oxygen-processed $\text{Y}_{0.33}\text{Sr}_{0.67}\text{CoO}_{3-\delta}$ were studied. The samples exhibit the perovskite-based structure with a space group of $I4/mmm$ (No. 139) and a layered ordering

of oxygen vacancies. The alternate layered order of CoO_6 octahedron and CoO_4 tetrahedral polyhedron and the intermediate spin $t_{2g}^5 e_g^1$ configuration result in the form of the orbital ordering state in the intermediate spin state of the Co^{3+} octahedron position. The orbital ordering appearance induces the nonmetal of both samples in whole temperature. Magnetic memory effect in about 200 K under 0.01 T is observed and related to the Co^{3+} spin state transition in the octahedral site from the intermediate to low spin state. The magnetization transition around 304 K is attributed to the competition of Co^{3+} antiferromagnetic and ferromagnetic interaction in the orbital ordering state. The air-processed $\text{Y}_{0.33}\text{Sr}_{0.67}\text{CoO}_{2.704}$ possesses the rich Co^{3+} ions due to the oxygen deficiency which supports the larger magnetization than that in the oxygen-processed $\text{Y}_{0.33}\text{Sr}_{0.67}\text{CoO}_{2.614}$. The rich Co^{3+} ions and the weak Co^{2+} and Co^{3+} interaction ac-

celerate the Jahn-Teller distortion to localize the e_g electron, which gives rise to the higher $T_J=204$ K in the air-processed $\text{Y}_{0.33}\text{Sr}_{0.67}\text{CoO}_{2.704}$. The oxides of the low oxidation states in the oxygen-processed $\text{Y}_{0.33}\text{Sr}_{0.67}\text{CoO}_{2.614}$ lead to a possible intermediate spin state stabilization due to the low distortion to low T_J . The observation of magnetic memory effect provides an experimental proof about the spin state transition of Co^{3+} ions in cobaltites.

ACKNOWLEDGMENTS

The authors would like to thank Fumiko Sakai and Youko Kiuchi (ISSP, Japan) for oxygen content measurement, and Ayako Yamamoto (RIKEN, Japan) for valuable advice to the result discussions.

-
- ¹R. Lengsdorf, M. Ait-Tahar, S. S. Saxena, M. Ellerby, D. I. Khomskii, H. Micklitz, T. Lorenz, and M. M. Abd-Elmeguid, *Phys. Rev. B* **69**, 140403(R) (2004).
- ²P. Ravindran, H. Fjellvag, A. Kjekshus, P. Blaha, K. Schwarz, and J. Luitz, *J. Appl. Phys.* **91**, 291 (2002).
- ³F. Fauth, E. Suard, and V. Caignaert, *Phys. Rev. B* **65**, 060401(R) (2001).
- ⁴M. Kriener, C. Zobel, A. Reichl, J. Baier, M. Cwik, K. Berggold, H. Kierspel, O. Zabara, A. Freimuth, and T. Lorenz, *Phys. Rev. B* **69**, 094417 (2004).
- ⁵J. Wu and C. Leighton, *Phys. Rev. B* **67**, 174408 (2003).
- ⁶S. Mukherjee, R. Ranganathan, P. S. Anilkumar, and P. A. Joy, *Phys. Rev. B* **54**, 9267 (1996).
- ⁷W. S. Kim, E. O. Chi, H. S. Choi, N. H. Hur, S.-J. Oh, and H.-C. Ri, *Solid State Commun.* **116**, 609 (2000).
- ⁸W. Kobayashi, S. Ishiwata, I. Terasaki, M. Takano, I. Grigoraviciute, H. Yamauchi, and M. Karppinen, *Phys. Rev. B* **72**, 104408 (2005).
- ⁹S. Ya. Istomin, J. Grins, G. Svensson, O. A. Drozhzhin, E. L. Kozhevnikov, E. V. Antipov, and J. P. Attfield, *Chem. Mater.* **15**, 4012 (2003).
- ¹⁰R. L. Withers, M. James, and D. J. Grossens, *J. Solid State Chem.* **174**, 198 (2003).
- ¹¹S. Roy, M. Khan, Y. Q. Guo, J. Craig, and N. Ali, *Phys. Rev. B* **65**, 064437 (2002).
- ¹²R. H. Potze, G. A. Sawatzky, and M. Abbate, *Phys. Rev. B* **51**, 11501 (1995).
- ¹³T. Vogt, P. M. Woodward, P. Karen, B. A. Hunter, P. Henning, and A. R. Moodenbaugh, *Phys. Rev. Lett.* **84**, 2969 (2000).
- ¹⁴M. James, D. Cassidy, D. J. Goossens, and R. L. Withers, *J. Solid State Chem.* **177**, 1886 (2004).
- ¹⁵M. James, D. Cassidy, K. F. Wilson, J. Horvat, and R. L. Withers, *Solid State Sci.* **6**, 655 (2004).
- ¹⁶M. A. Korotin, S. Yu. Ezhov, I. V. Solovyev, V. I. Anisimov, D. I. Khomskii, and G. A. Sawatzky, *Phys. Rev. B* **54**, 5309 (1996).
- ¹⁷F. Izumi and T. Ikeda, *Mater. Sci. Forum* **198**, 321 (2000).
- ¹⁸M. Karppinen, M. Matvejeff, K. Salomäki, and H. Yamauchi, *J. Mater. Chem.* **12**, 1761 (2002).
- ¹⁹Y. F. Zhang, S. Sasaki, O. Yanagisawa, and M. Izumi (unpublished).
- ²⁰D. J. Goossens, K. F. Wilson, M. James, A. J. Studer, and X. L. Wang, *Phys. Rev. B* **69**, 134411 (2004).
- ²¹A. A. Taskin, A. N. Lavrov, and Yoichi Ando, *Phys. Rev. B* **71**, 134414 (2005).
- ²²L. D. Tung, *Phys. Rev. B* **73**, 024428 (2006).
- ²³Guixin Cao, Jincang Zhang, Shixun Cao, Chao Jing, and Xuechu Shen, *Phys. Rev. B* **71**, 174414 (2005).
- ²⁴K. Liu, X. W. Wu, K. H. Ahn, T. Sulchek, C. L. Chien, and J. Q. Xiao, *Phys. Rev. B* **54**, 3007 (1996).
- ²⁵*Colossal Magnetoresistance Oxides*, edited by Y. Tokura (Gordon & Breach Science Publishers, London, 1999).
- ²⁶M. A. Senarís-Rodríguez and J. B. Goodenough, *J. Solid State Chem.* **118**, 323 (1995).
- ²⁷P. S. Anil-Kumar, P. A. Joy, and S. K. Date, *J. Phys.: Condens. Matter* **10**, L487 (1998).
- ²⁸G. Maris, Y. Ren, V. Volotchaev, C. Zobel, T. Lorenz, and T. T. M. Palstra, *Phys. Rev. B* **67**, 224423 (2003).
- ²⁹Y. P. Chernenkov, V. P. Plakhty, V. I. Fedorov, S. N. Barilo, S. V. Shiryayev, and G. L. Bychkov, *Phys. Rev. B* **71**, 184105 (2005).
- ³⁰A. A. Taskin, A. N. Lavrov, and Y. Ando, *Phys. Rev. Lett.* **90**, 227201 (2003).
- ³¹D. I. Khomskii and K. I. Kugel, *Solid State Commun.* **13**, 763 (1973).
- ³²Y. Tokura and N. Nagaosa, *Science* **288**, 462 (2000).